Communication

Self-Assembly of Chiral Molecular Honeycomb Networks on Au(111)

Wende Xiao, Xinliang Feng, Pascal Ruffieux, Oliver Gro#ning, Klaus Mu#llen, and Roman Fasel

More About This Article

Additional resources and features associated with this article are available within the HTML version:

- Supporting Information
- Links to the 1 articles that cite this article, as of the time of this article download
- Access to high resolution figures
- Links to articles and content related to this article
- Copyright permission to reproduce figures and/or text from this article

View the Full Text HTML

ACS Publications
High quality. High impact.

Self-Assembly of Chiral Molecular Honeycomb Networks on Au(111)

Wende Xiao,[†] Xinliang Feng,[‡] Pascal Ruffieux,[†] Oliver Gröning,[†] Klaus Müllen,*,[‡] and
Roman Fasel*,[†]

*Empa, Swiss Federal Laboratories for Materials Testing and Research, Feuerwerkerstrasse 39, CH-3602 Thun,
Switzerland, and Max-Planck-Institute for Polymer Research, Ackermannweg 10, 55128 Mainz, Germany*

Received December 21, 2007; E-mail: muellen@mpip-mainz.mpg.de; roman.fasel@empa.ch

In recent years, the transfer and adaptation of the concepts of crystal engineering[1] to the case of two-dimensional (2D) molecular self-assembly on solid surfaces has intensively been explored.[2] The formation of a variety of well-defined, 2D porous molecular networks based on specific, noncovalent interactions such as hydrogen bonding (HB), dipolar coupling, and metal co-ordination has been reported.[3] Such regular open networks offer the possibility to host functional guest molecules in a controllable way, with potential applications in single-molecule-based devices.

Hexaphenylbenzene (HPB) is one of the smallest rigid star-shaped polyphenylenes, and has recently been designed to engineer porous crystals.[4] Surface patterning with HPB has only rarely been investigated,[5] presumably due to a lack of HPB derivatives exhibiting appropriate molecular symmetry and functionality. Herein, we report on the formation of surface-supported chiral honeycomb networks by self-assembly of a novel, specifically designed C_3 symmetric 1,3,5-trikis(4′-carboxylphenyl)-2,4,6-trikis(4′-tert-butylphenyl)-benzene (**1**, Figure 1a) on the Au(111) surface. In-situ ultrahigh vacuum scanning tunneling microscopy (STM) investigations and force field calculations show that **1** self-assembles into a series of 2D hexagonal porous networks, where molecules of **1** within each half-unit cell are close-packed via van der Waals (vdW) interactions, and all half-unit cells are connected to each other via dimeric HBs between carboxyl groups. Asymmetric molecular close-packing within the half-unit cells induces chirality in the honeycomb networks. The coexistence of various honeycomb orders at submonolayer coverages highlights the importance of both specifically designed directional interactions (Desiraju–Wuest postulate)[1b,c] and weaker, less specific interactions such as vdW that favor close-packing (Kitaigorodskii's principle)[6] in determining 2D crystal structures.

Molecule **1** consists of a HPB core and three alternating *tert*-butyl spacer and carboxyl groups. In the solid state and on surfaces, the outer phenyl rings of the HPB core are rotated around their σ-bonds connecting to the central benzene ring because of intramolecular steric hindrance, resulting in a dihedral angle of ∼65°.[4] Because of the resulting propeller shape of the HPB core, surface-adsorbed **1** has two opposite chiral conformations. We note that the handedness of single molecules is intrinsic and its definition requires no consideration of the molecule−surface system (see Supporting Information). The inert Au(111) surface is chosen as the substrate, so that molecule−surface interactions are minimized and the self-assembly of **1** is expected to be mainly guided by the specifically designed intermolecular interactions.

After vapor deposition of 0.3 monolayer (ML) **1** onto clean Au(111) at room temperature (RT) and subsequent annealing to temperatures between 100−180 °C, we observe by STM a variety
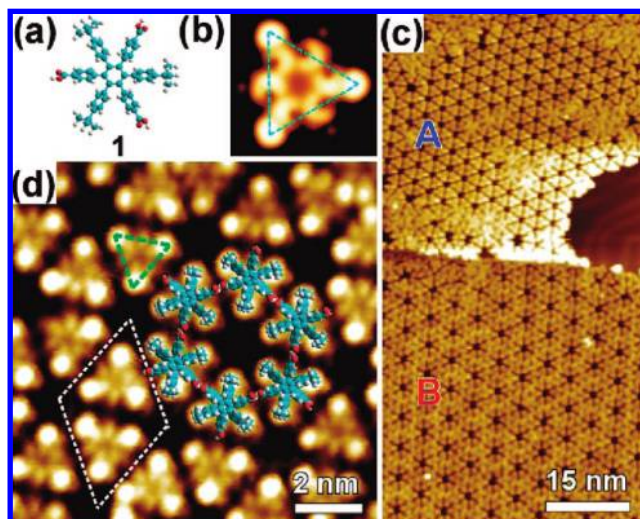

Figure 1. STM images after rt deposition of 0.3 ML **1** on Au(111) followed by annealing to 100−180 °C: (a) ball-and-stick model of **1**; (b) EHT-STM simulation of **1**; (c) overview image showing coexistence of two different ordered phases A and B; (d) details of the ordered honeycomb network structure of phase A. The unit cell of the honeycomb network is marked with dashed lines.

of ordered phases as well as some disordered structures at a sample temperature of ∼50 K, as demonstrated in Figure 1c. Images at high magnification (Figure 1d) of phase A show a regular honeycomb lattice with a pore-to-pore distance of 2.96 ± 0.05 nm. Each unit cell consists of two molecules, and each molecule resembles an equilateral triangle with the three brightest spots originating from the three *tert*-butyl spacers. In highly resolved images such as the one shown in Figure 1d, the six phenyl rings of the HPB core can be identified as fainter intensity maxima. STM image simulations based on semiempirical extended Hückel theory (EHT) support this interpretation of the experimental STM images of **1**, as demonstrated in Figure 1b.

Amber3 force field calculations (see Supporting Information) reveal that the formation of the phase A honeycomb network is driven by the maximization of HBs, namely, the formation of three dimeric HBs for each molecule with its three nearest neighbors via carboxyl groups. Since the carboxyl groups prefer to stay in the plane of the connecting phenyl rings, the formation of dimeric HBs is only possible between molecules of opposite handedness. Therefore, the honeycomb network observed in phase A is overall racemic. We denote it as HC_1, where HC stands for the honeycomb network of **1**, and the subscript number 1 indicates that the side length of the triangular half-unit cell is one molecule. The corresponding structural model is superposed to Figure 1d (see also Figure 3a). Similar structures have been observed for other C_3
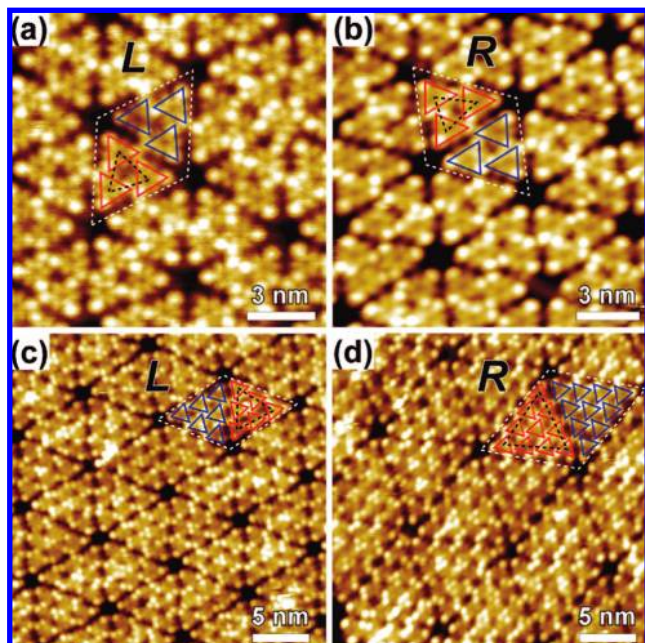
Figure 2. STM images of ordered chiral honeycomb networks observed after deposition of 0.3 ML **1**: (a, b) *L*- and *R*-domains of the HC_2 structure; (c) *L*-domain of the HC_3 structure; (d) *R*-domain of the HC_4 structure. Unit cells are indicated by white dashed lines. Individual molecules are schematically indicated as red and blue triangles (opposite chiral conformations of **1**) with corners at *tert*-butyl positions.

symmetric molecules, such as trimesic acid (TMA) or 1,3,5-benzenetribenzoic acid.[7,8]

Phase B also exhibits a honeycomb lattice, but with a periodicity of 4.63 ± 0.05 nm, much larger than that of phase A. Each unit cell again consists of two triangular subunits (half-unit cells), which, however, are not single molecules but trimers of **1** with an intermolecular separation of 1.7 ± 0.05 nm, as seen in the close-ups shown in Figure 2(a,b). The orientation of the triangle constructed by connecting the centers of mass of three molecules inside a subunit is rotated by $\pm 15°$ with respect to the triangular molecular configurations. We denote this honeycomb network as HC_2 because its triangular subunit has a side length of two molecules. Force field calculations give an equilibrium intermolecular separation of 1.72 nm for the trimer and a molecular arrangement in perfect agreement with the one derived from STM images such as Figure 2(a,b). The three molecules of **1** inside a subunit have the same handedness and are close-packed via vdW interactions. As for the HC_1 structure, the subunits are bound to each other via dimeric HBs between carboxyl groups, implying that molecules in the two different subunits of a unit cell have opposite handedness. Therefore, the HC_2 network is racemic from a molecular point of view. On the other hand, asymmetric close-packing of the three molecules within the half-unit cells leads to chiral trimer subunits, as illustrated in Figure 2(a,b).[9] The trimers in the two half-unit cells have identical molecular arrangements, but with an in-plane rotation of 180°. The chirality of the trimer subunits is thus transferred to the unit cell and to the entire honeycomb network. Extended homochiral domains of both the left-handed (*L*) and the right-handed (*R*) honeycomb network HC_2 are observed (Figure 2(a,b)). A structural model of the *L*-domain of the HC_2 network is illustrated in Figure 3b.[9]

The HC_2 structure can be viewed as an inflation of the HC_1 structure by addition of one more row (with two molecules) into its half-unit cell. Generalizing this view, higher order honeycomb networks HC_{n+1} can be obtained by appending a row of $n+1$
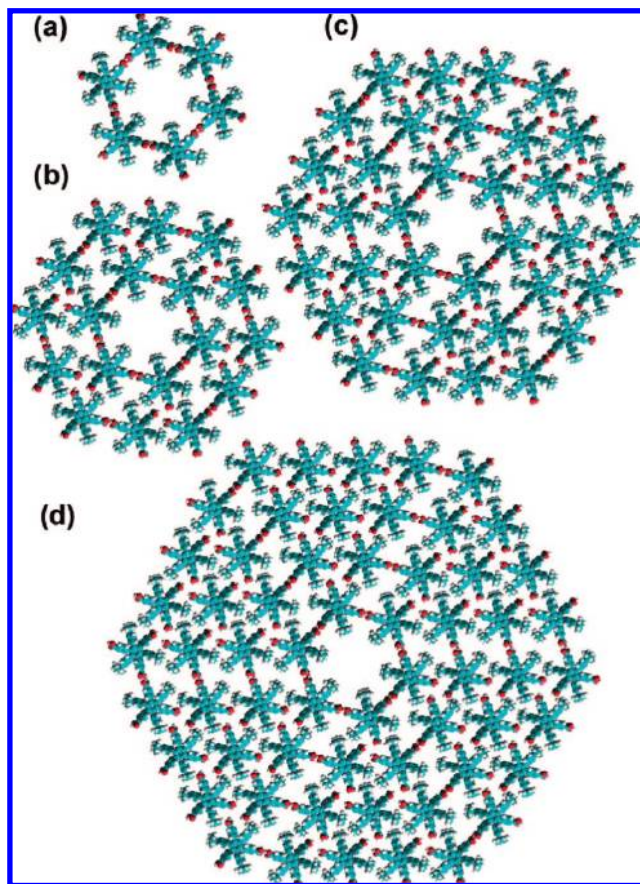

Figure 3. Structural models of the honeycomb networks of **1**. (a) HC_1 structure. (b–d) *L*-domains of the HC_2, HC_3, and HC_4 structures, respectively.

molecules to each half-unit cell of the HC_n structure ($n = 1, 2, 3, ..., \infty$). The molecules inside a half-unit cell are close-packed via vdW interaction, forming a chiral triangle, while the half-unit cells are bound to each other via n HBs. The pore-to-pore distance d_n of the HC_n structure can be described by $d_n = (n - 1)p + q$, where $q = 2.96$ nm is the interpore distance of the HC_1 structure, and $p = 1.7$ nm is the intermolecular distance of the close-packed monolayer (which can be regarded as the HC_∞ structure with infinite interpore distance). We indeed observe highly ordered chiral domains of the HC_3 and HC_4 structures (Figure 2(c,d)), as well as extended close-packed domains (HC_∞). Structural models for the *L*-domains of the HC_3 and the HC_4 structures are given in Figure 3(c,d). The measured interpore distances of the HC_3 and HC_4 structures are 6.4 ± 0.05 and 8.05 ± 0.05 nm, respectively, well consistent with the values expected from the generalized model. Local patches corresponding to even higher order HC_n structures with $n = 5, 6, 7,$ and 8 are also observed, but with relatively poor long-range order.

The formation of a series of honeycomb networks with increasing interpore distance is not limited to **1**. During the completion of this manuscript, a similar behavior was reported for TMA on Au(111): Depending on the TMA coverage, honeycomb networks with half-unit cells containing molecules in up to 8 rows were observed.[8] Comparing the self-assembly of **1** and TMA molecules, it is obvious that in both cases the half-unit cells are strongly bound to each other via dimeric HBs, while the molecules within the half-unit cells are close-packed via weaker interactions (trimeric HBs for the TMA molecules and vdW interactions for **1**). Notably, the TMA honeycomb networks are achiral, while the ones of **1** are
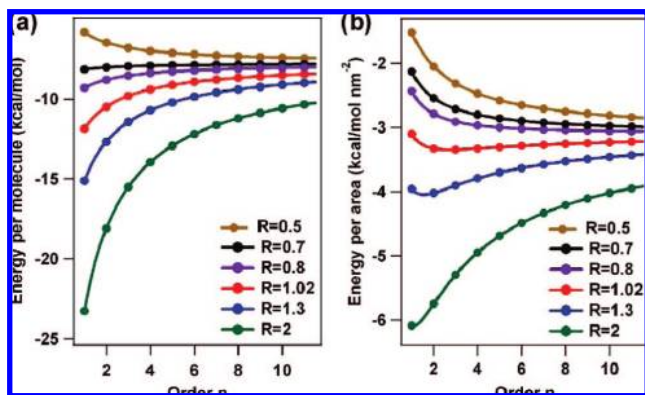
Figure 4. (a) Interaction energy per molecule (E_n^{mol}) vs the order (n) of the honeycomb networks of **1**. (b) Interaction energy density (E_n^A) vs the order (n) of the honeycomb networks of **1**. Different ratios (R) of the interaction energy of dimeric hydrogen bonds to that of a close-packed trimer are plotted. The red curves with $R = 1.02$ correspond to the actual interaction energy values as obtained from Amber3 force field calculations.

chiral due to the asymmetric molecular close-packing inside half-unit cells. Generally, we propose that if a molecule with C_3 symmetry can form both a honeycomb network via a strong and directional binding and a hexagonal close-packed structure via a weaker interaction, it will also be able to self-assemble into a series of higher order honeycomb network structures with increasing interpore distance.

In the case of TMA, the formation of higher order honeycomb networks with increasing coverage is understood from simple H-bond optimization considerations.[8] In the present case of the HPB species **1**, however, the coexistence of various honeycomb orders at submonolayer coverages calls for a more elaborate explanation. We have investigated the energetics of the HC$_n$ family of honeycomb networks by means of molecular force field calculations (see Supporting Information). For a honeycomb network HC$_n$ of order n, the total interaction energy per molecule is given by $E_n^{mol} = (3nE_{HB} + n(n-1)E_{CP})/(n(n+1))$, where E_{HB} and E_{CP} refer to the energy gains of forming a dimeric HB and a close-packed trimer, respectively. The resulting interaction energy as a function of order n is shown in Figure 4a. The red curve corresponds to a ratio $R = E_{HB}/E_{CP}$ of 1.02 between the dimeric hydrogen-bonding and trimeric close-packing interaction energies as given by Amber3 force field calculations ($E_{HB} = -7.9$ kcal/mol; $E_{CP} = -7.75$ kcal/mol; see Supporting Information). According to this interaction energy per molecule curve, submonolayers of **1** should obviously condense exclusively in the strongly favored order 1 network HC$_1$, which is contrary to experimental observations. Kinetic limitations are not able to explain the formation of higher order networks, since they are expected to act in the opposite direction, that is, to hinder the formation of higher order, more complex structures.

The situation looks different if we consider the total interaction energy *density* $E_n^A = (3nE_{HB} + n(n-1)E_{CP})/\sqrt{3/2}d_n^2$, that is, the interaction energy per unit area. The resulting interaction energy density curves for different E_{HB}/E_{CP} ratios R are shown in Figure 4b. For the ratio $R = 1.02$ corresponding to our calculated interaction energy strengths, the interaction energy density depends only weakly on the order n of the network, and exhibits a minimum for $n = 2{\sim}3$. Higher order networks ($n = 4, 5,...$) are only slightly less favorable. The near degeneracy of the interaction energy density for order 2, 3,..., 8 honeycomb networks thus rationalizes the experimentally observed coexistence of these different honeycombs of **1**.

In being rationalized in terms of interaction energy *densities* rather than interaction energies per molecule, our results suggest that Kitaigorodskii's principle of closest-packing might also apply to 2D molecular systems.[6] They indicate that considering interaction energies per molecule might not be sufficient to determine lowest-energy configurations of 2D molecular systems: Intrinsically stronger intermolecular association (favoring low order honeycombs) may be counterbalanced by tighter packing (favoring higher order honeycombs). A similar conclusion has been drawn for 3D crystallization by Angeloni and co-workers: When determining the three-dimensional crystal structures of a series of $[PtCl_4]^{2-}$ and $[SbCl_5]^{2-}$ salts,[10] they found that local HB interactions, although important in determining the local intermolecular geometry, are not the only or even the decisive influence on the crystal structures. The close-packing of the complex ions also plays an important role, and the crystal structures of these molecular salts result from the subtle balance of directional HBs and close-packing. Similarly, our results provide a 2D example where both, the Desiraju−Wuest postulate and Kitaigorodskii's principle of closest packing, play important roles in determining molecular crystal structures.[1,6]

In summary, we have investigated the self-assembly of the novel C_3 symmetric star-shaped molecule **1** on a Au(111) surface at the submolecular level by STM. We observe a variety of chiral honeycomb structures where molecules inside half-unit cells are close-packed via vdW interactions while half-unit cells are connected to each other via dimeric HBs between carboxyl groups. The networks are chiral due to nonsymmetrical molecular close-packing inside the half-unit cells. The coexistence of various honeycomb orders highlights the subtle interplay of directional HB and less specific vdW interactions in determining 2D crystal structures.

Supporting Information Available: Synthesis and characterization of compounds, STM experiments, molecular modeling, chirality of surface-adsorbed **1**, and force field calculations. This material is available free of charge via the Internet at http://pubs.acs.org

References

(1) (a) Schmidt, G. M. J. *Pure Appl. Chem.* **1971**, *27*, 647. (b) Desiraju, G. R. *Angew. Chem., Int. Ed.* **1995**, *34*, 2311. (c) Su, D.; Wang, X.; Simard, M.; Wuest, J. D. *Supramol. Chem.* **1995**, *6*, 171.
(2) Barth, J. V. *Annu. Rev. Phys. Chem.* **2007**, *58*, 375.
(3) (a) Theobald, J. A.; Oxtoby, N. S.; Phillips, M. A.; Champness, N. R.; Beton, P. H. *Nature* **2003**, *424*, 1029. (b) Stepanow, S.; Lingenfelder, M.; Dmitriev, Al; Spillmann, H.; Delvigne, E.; Lin, N.; Deng, X.; Cai, C.; Barth, J. V.; Kern, K. *Nat. Mater.* **2004**, *3*, 229. (c) Pawin, G.; Wong, K. L.; Kwon, K.-Y.; Bartels, L. *Science.* **2006**, *313*, 961.
(4) (a) Maly, K. E.; Gagnon, E.; Maris, T.; Wuest, J. D. *J. Am. Chem. Soc.* **2007**, *129*, 4306. (b) Kobayashi, K.; Sato, A.; Sakamoto, S.; Yamaguchi, K. *J. Am. Chem. Soc.* **2003**, *125*, 3035. (c) Kobayashi, K.; Shirasaka, T.; Sato, A.; Horn, E.; Furukawa, N. *Angew. Chem., Int. Ed.* **1999**, *38*, 3483.
(5) (a) Gross, L.; Rieder, K. H.; Moresco, F.; Stojkovic, S. M.; Gourdon, A.; Joachim, C. *Nat. Mater.* **2005**, *4*, 892. (b) Gross, L.; Moresco, F.; Ruffieux, P.; Stojkovic, S. M.; Gourdon, A.; Joachim, C.; Rieder, K. H. *Phys. Rev. B* **2005**, *71*, 165428.
(6) Kitaigorodskii, A. I. *Acta Crystallogr.* **1965**, *18*, 585.
(7) (a) Griessl, S.; Lackinger, M.; Edelwirth, M.; Hietschold, M.; Heckl, W. M. *Single Mol.* **2002**, *3*, 1. (b) Ruben, M.; Payer, D.; Landa, A.; Comisso, A.; Gattinoni, C.; Lin, N.; Collin, J.-P.; Sauvage, J.-P.; De Vita, A.; Kern, K. *J. Am. Soc. Chem.* **2006**, *128*, 15644.
(8) Ye, Y.; Sun, W.; Wang, Y.; Shao, X.; Xu, X.; Cheng, F.; Li, J.; Wu, K. *J. Phys. Chem. C.* **2007**, *111*, 10138.
(9) See the Supporting Information for detailed molecular models of the L- and R-domains of the HC$_2$ structure.
(10) Angeloni, A.; Crawford, P. C.; Orpen, A. G.; Podesta, T. J.; Shore, B. J. *Chem. Eur. J.* **2004**, *10*, 3783.

JA7106542